Catalysis Letters Vol. 111, Nos. 3–4, November 2006 (© 2006)
DOI: 10.1007/s10562-006-0138-3

Titania and titania-silver nanoparticle deposits made by Liquid Flame Spray and their functionality as photocatalyst for organic- and biofilm removal

Helmi Keskinen,[a,*] Jyrki M. Mäkelä,[a] Mikko Aromaa,[a] Jorma Keskinen,[a] Sami Areva,[b] Cilâine V. Teixeira,[b] Jarl B. Rosenholm,[b] Viljami Pore,[c] Mikko Ritala,[c] Markku Leskelä,[c] Mari Raulio,[d] Mirja S. Salkinoja-Salonen,[d] Erkki Levänen,[e] and Tapio Mäntylä[e]

[a,*]*Institute of Physics, Tampere University of Technology, P.O. Box 692, FIN-33101 Tampere, Finland*
[b]*Department of Physical Chemistry, Åbo Akademi University Porthansgatan 3–5, FIN-20500 Turku, Finland*
[c]*Laboratory of Inorganic Chemistry, Department of Chemistry University of Helsinki, P.O. Box 55, FIN-00014 Helsinki, Finland*
[d]*Department of Applied Chemistry and Microbiology, University of Helsinki, P.O. Box 56, FIN-00014 Helsinki, Finland*
[e]*Institute of Material Sciences, Tampere University of Technology, P.O. Box 589, FIN-33101 Tampere, Finland*

Received 18 April 2006; accepted 2 September 2006

Titania and titania-silver nanoparticle deposits were made by Liquid Flame Spray technique, in which the liquid precursor is injected into a high temperature flame, where it will evaporate and nucleate to nanosize particles. One-step and two-step methods were used for preparation of titania-silver deposits. The amount of silver added was 1 wt%. The deposits were collected in the flame zone on steel and glass surfaces and were analyzed by TEM, EDS, XPS and SAXS. The titania deposits consisted of porous nanosized titania agglomerates of primary particles (~10 nm). With silver addition, small spherical silver metal particles (~2 nm) were detected on the agglomerates. An increase in the photocatalytic activity was verified by stearic acid decomposition and biofilm removal using *Deinococcus geothermalis* as the model organism.

KEY WORDS: liquid flame spray; deposits; photocatalyst; titanium dioxide.

1. Introduction

Flame methods have been used in particle production for several decades [1]. Most of the present studies in this area concentrate on multicomponent nanoparticles or deposits production [2–12]. Titania is well known for its photocatalytic properties [13–15]. Addition of silver to titania has been proved to increase this activity [16,17]. In bacterial studies silver has been also noticed to have an increasing effect on biofilm removal [18]. The advantages of the flame method are process speed, cost effectiveness and possibility of scaling up to industrial quantities [19]. In Liquid Flame Spray (LFS) [20], the liquid precursor is injected into a high temperature flame (T_{max}~3000 °C), where it will evaporate and nucleate to nanosize particles. The potential of producing titania [21,22] and titania/silver [12] nanoparticles and deposits by this method were studied recently. In these recent studies also particle deposition mechanism and particle morphology were studied [12, 21, 22]. In this study, photocatalytically active titania and titania-silver deposits for different substrates were produced by LFS. The amount of silver added was 1 wt%. Two methods (one-step, two-step) for producing titania-silver deposits were used. The objectives of this study were to characterize morphology of the deposits and their capability for photocatalytic stearic acid decomposition and for biofilm removal. Especially the effect of silver addition by one-step/two-step method to photocatalytic activity was highlighted.

*To whom correspondence should be addressed.

2. Experimental

2.1. Preparation of deposits

In the LFS method a turbulent, high-temperature H_2–O_2 flame was used. The gas flow rates used were 20 L/min for H_2 and 10 L/min for O_2 and the maximum temperature was ~3000 °C [20]. The liquid precursor was atomized into small droplets by the high velocity H_2 flow. The droplets are then introduced into the flame where they evaporate. After evaporation they decompose and the reaction product re-condenses into product species. This process generates well-defined nanoparticles which can be sprayed on a surface or collected as a powder [12, 21, 22]. Titanium(IV)ethoxide (TEOT) and silver nitrate ($AgNO_3$) in ethanol solution were selected as the precursors. All samples (A–J) for different analyzes (XPS, SAXS etc.) are presented in table 1. The deposits were collected directly from the flame by wiping

the substrates vertically to the flame (A, B, E–L). The powder samples (C, D) were collected at a longer distance from the flame by an electrostatic precipitator. Titania-silver powder or deposit was produced by a one-step or a two-step method. In the two-step method the titania particles were generated first (table 1; B, D, G, J and L) and after that the produced layer of titania was coated by silver particles. In the one-step method a mixed single precursor (table 1; A, C, F, I and K) was used. The mass flow rate for titania was kept at 40 mg/min and for silver at 0.4 mg/min. It is known from recent studies that by these mass flow rates titania agglomerates consisting of ~10 nm primary particles and ~2 nm spherical silver nanoparticles are produced [12,22]. It is also observed that the deposits collection time and temperature influence on the deposit porosity and particle size because of sintering of the particles [21]. Therefore, it is expected that samples A–D are denser and have larger particle size than samples E–L.

2.2. Characterization of deposits

For the studies of morphology and chemical composition Transmission Electron Microscopy (TEM), Energy Dispersive Spectroscopy (EDS), X-ray Photoelectron Spectroscopy (XPS) and small-angle X-ray scattering (SAXS) were used. The TEM (JEM 2010 from JEOL, Tokyo, Japan) equipped with an EDS, Model Noran Vantage from ThermoNoran (The Netherlands) were used (samples K and L). Samples A and B were analyzed by XPS. XPS-spectra were recorded using a Physical Electronics Quantum 2000 ESCA instrument. The XPS measurements were performed at a base pressure of 1×10^{-9} Torr using an AlK_{α} X-ray source. The pass energies for low and high-resolution spectral acquisition were 117.4 and 23.3 eV, respectively. The powder samples C and D were studied with small-angle X-ray scattering (SAXS), with a Kratky compact camera, with a Seifert ID-3003 X-ray generator operating at a maximum of 50 kV/40 mA. CuK_{α} radiation was used. The system was equipped with a position-sensitive detector consisting of 1024 channels of 55.9 mm each and sample-detector distance of 277 mm. The detector calibration was made with Silver Behenate (d-spacing = 58.38 Å). The camera was kept in vacuum in order to minimize the scattering from the air. The powders were measured in glass capillaries of an external diameter of 2 mm. Before filling the capillary with the sample, the scattering curve of the empty capillary was obtained and used as the background, which was subtracted from the measured curve.

Stearic acid ($CH_3(CH_2)_{16}CO_2H$, Aldrich, 95%) was used as a probe molecule to study the photocatalytic activity of the samples (E–G). A comparison study for durability of deposits was also done with samples which were systematically rinsed with ethanol and wiped by lint-free cloth in an effort to remove loosely adhered deposit. The stearic acid coated samples were irradiated by UV light (λ = 365 nm, intensity = 0.9 mW/cm^2) and the degradation of stearic acid was monitored by FTIR spectroscopy. The test procedure is described in more detail elsewhere [23].

The model bacterium used for the photocatalytic biofilm destruction studies was *Deinococcus geothermalis* E50051 (HAMBI 2411) [24]. All samples were

Table 1
Experimental conditions for sample preparation

Sample	Collecting method	Substrate	Titania (mg/min)	Silver (mg/min)	Distance (cm)	Time (s)
XPS studies						
A	deposit (one-step)	steel plate	40	0.4	15	1200
B	deposit (two-step)	steel plate	40		15	1200
B		steel plate (+titania)		0.4	15	1200
SAXS studies						
C	powder (one-step)		40	0.4	30	1500
D	powder (two-step)		40		30	1500
D				0.4	30	1500
Stearic acid degradation						
E	deposit	glass plate	40		5	20
F	deposit (one-step)	glass plate	40	0.4	7	20
G	deposit (two-step)	glass plate	40		7	20
G		glass plate (+titania)		0.4	7	20
Biofilm reduction						
H	deposit	steel plate	40		5	20
1	deposit (one-step)	steel plate	40	0.4	5	20
J	deposit (two-step)	steel plate	40		5	20
J		Steel plate (+titania)		0.4	5	20
TEM studies						
K	deposit (one-step)	TEM-grid	40	0.4	15	10
L	deposit (two-step)	TEM-grid	40		15	10
L		TEM-grid (+titania)	40	0.4	15	10

disinfected (70% ethanol) and mounted in the wells of a polystyrene plate. The wells were filled with 3 mL of culture medium (oligotrophic medium R2 [25]) and inoculated with 5 vol% of *D. geothermalis*-strain E50051 grown for 1 d under shaking in R2 broth. The plate was covered with a lid and incubated under shaking (160 rpm) for 2 d at +45 °C in the dark. The plates holding samples with pre-grown biofilms, submerged in the water (3 mm liquid above the biofilm), were illuminated (Sylvania 18 W Blacklight Blue) or not illuminated (control) at 360 nm, 0.1 mW/m^2, for 24 h, under shaking at +45 °C.

Cell density of *D. geothermalis* of the biofilms was measured as described by Raulio *et al.* [26,27]. Briefly, the test coupons were flooded with the fluorochrome dye (SYTO9, Molecular Probes, Leiden, Netherlands) that has affinity to bacteria and emits specific fluorescence only when bound to cellular DNA or RNA. The emitted fluorescence cm^{-2} of test coupon was quantified by scanning fluorometer (Nikon Eclipse E800, Tokyo, Japan). The fluorochrome emission was calibrated with preparations containing known numbers of *D. geothermalis* cells.

3. Results and discussion

3.1. Deposits morphology and composition

In principle, four different morphology possibilities for titania-silver deposits can be considered. These possibilities are illustrated in figure 1. In the choice A the silver and titania are uniformly distributed in the particles, titania particles are doped via silver atoms inside the titania crystal lattice. In another possibility B the titania particles are uniformly coated by thin silver film. The particles can also be separated like in choice C, where there are titania particles covered by smaller silver particles through whole deposit or the silver particles can be concentrated to the topmost layer of the deposit (choice D).

The corrected SAXS curves obtained for both samples are shown in figure 2. For both samples, the curves show only the direct beam, without any additional scattering. The difference in number of electrons between Ti (22 electrons) and Ag (47 electrons) is very high, which means we would certainly observe a well-defined scattering curve typical of spherical particles with two different electron densities. The absence of scattering in the curves indicates homogeneity in electron density in the particles, which means that the particles are equally distributed in the sample, which excludes the possibility of the morphology in figure 1(b). As only few silver particles are distributed, randomly, on the titania particles, it is difficult to obtain enough intensity for the scattering, so, although no intensity was observed, the morphologies in figures 1(a), (c), and (d) cannot be excluded. From the wide scan XPS spectra only oxygen, titanium, silver and some traces of adventitious carbon were detected. The binding energies (BEs) were referenced to that of the adventitious carbon 1 s peak at 285.0 eV. The Ag/Ti ratio was calculated from the fitted high-resolution spectra. For the sample A (one-step) the percentual ratio of Ag/(Ag + Ti) was 11.4% and for sample B (two-step) 43.7%. Silver is highly enriched on the surface in the two-step method (figure 1(d)) compared to the one-step (figure 1(c)) method as expected. The O(1 s) peaks appear at 530.3 (±0.3 eV) and the Ti (2 $p_{3/2}$) peaks at 459.1 (±0.2 eV) corresponding to TiO_2. The Ag (3 $d_{5/2}$) peaks appear at 368.3 (±0.2 eV), and the splitting of the 3 d doublet is 6.0 eV. These values correspond to metallic silver. These XPS results indicated that the morphology choice A can be also excluded, because no bond was detected between titanium and silver [12].

The TEM-micrographs from the two-step (sample L in table 1) and one-step (sample K n table 1) deposits are presented in figure 3. In the samples titanium, oxygen and

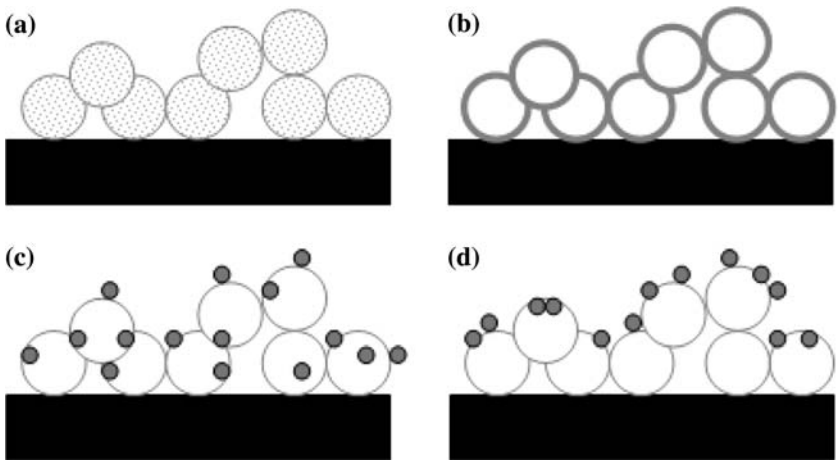

Figure 1. Morphology possibilities for titania particles (a) doped by silver, (b) coated by silver thin layer, (c) coated uniformly by silver particles and (d) the topmost layer coated by silver particles [12].

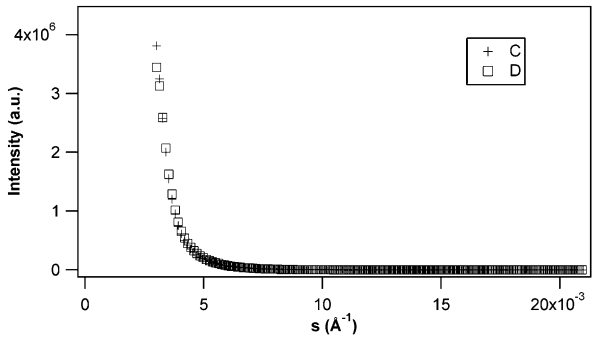

Figure 2. SAXS curves of titania-silver powders (one-step (c) and two-step (d)). The scattering vector s = 2d sin θ/λ, where 2θ is the scattering angle and λ is the wavelength of the CuK_α = 1.542 Å.

silver were detected by EDS. All these studies support recent studies on particle morphology [12]. The deposits consist of titania agglomerates (mostly anatase, [12, 21, 22]) with mean primary particle diameter (dp) ~10 nm [12]) coated by smaller spherical silver particles (dp~2 nm [12]). In the two-step method, silver is segregated highly on the topmost layer (figures 1(d) and 3(a)). In the one-step method, silver is dispersed more uniformly on the surface of the agglomerates in the whole deposit (figure 1(c) and 3(b)). In this recent study [12] also titania particle size have been reported decreasing (~10%) in one-step method with silver doping.

3.2. Photocatalytic activity

Photocatalytic activity of the samples was evaluated by the degradation of a thin layer of stearic acid. This reaction is widely used in the testing of photocatalytic surfaces and has been well characterized in the literature [28–33]. Although small amounts of side-products may exist during the degradation, the overall reaction can be written as:

$$CH_3(CH_2)_{16}CO_2H + 26O_2 \xrightarrow[h\nu \geq 3.2eV]{TiO_2} 18CO_2 + 18H_2O \quad (1)$$

In this work, the amount of degraded stearic acid was quantified from IR measurements according to Mills and Wang [28] and initial formal quantum efficiencies (FQE) were calculated for each sample. The FQE values simply indicate how many stearic acid molecules were destroyed per one incident photon. The initial FQE values for all samples are listed in table 2. The FQE values were quite high for the samples from which the loosely adhered deposits had not been removed. These deposits consisted of a powdery material with a large surface area, which of course explains the high activities. Samples were also tested after removing the loosely adhered particles (table 2). It can be seen that especially samples E and F had a noticeable activity after removing the loose particles, indicating that some TiO_2 still remained on the surface. The loose material morphology has been studied in previous paper [12] and it was similar as deposits here. There should not be much difference in the intrinsic activity between loose and adherent particles. There are simply much less active sites after the removal of loose particles for the photocatalytic reactions to occur and the activity per cm^2 is weaker. The sample produced by one-step method (F in table 2) seems to have the highest photocatalytic activity before removing the loose particles. Similar efficiencies for sol-gel derived TiO_2 coatings have been published earlier [29]. After removing the loose particles, sample E had the highest activity. The shorter collection distance during the deposition of sample E might have made the particles more adherent (table 1). The complete mineralization of stearic acid involves 104 electrons [28]. The FQE values in Table X can thus be multiplied by 104 when quantum efficiencies on an electron/incident photon basis are desired.

The tendency of the three deposits (samples H, I and J in table 1) to attract biofilm bacteria was compared to that of the non-coated steel substratum. The results are shown in figure 4. In absence of illumination less biofilm was attracted by the deposit coated surfaces than non-coated steel. The one- and two-step titania-silver deposits (samples I and J) attracted only $3–11 \times 10^6$ cells cm^{-2}

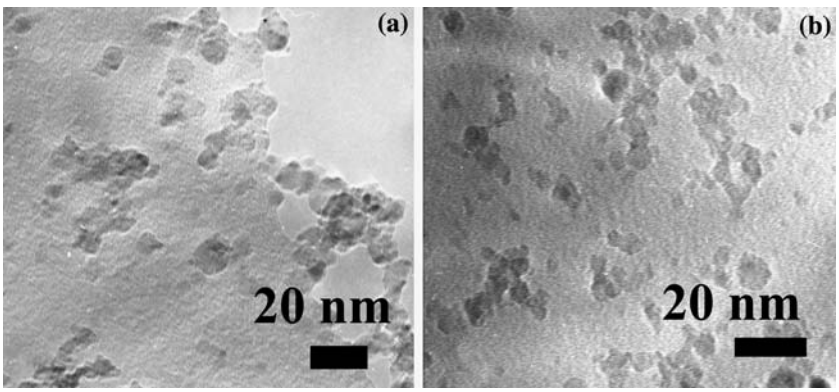

Figure 3. TEM-micrographs of deposits for two-step (a) and one-step (b) titania samples collected (collecting time 10 s) to TEM grid at 15 cm from the burner face.

Table 2
Initial formal quantum efficiencies for the degradation of stearic acid for titania (E), one-step titania-silver (F) and two-step titania-silver (G) deposits ((r) corresponds the values after removing loose particles)

Sample	FQE/10^{-3}
E	1.00
E (r)	0.048
F	1.09
F (r)	0.038
G	0.21
G (r)	0.0079

of bacteria as compared to the plain steel with 26×10^6 adhered cells cm^{-2}. After illumination, there remained only $0.2–2 \times 10^6$ cells cm^{-2} on the coated samples I and J. Illumination of titania (H) and one-step titania-silver (I) deposits removed 97% and 94% of the biofilm bacteria as compared to their non-illuminated counterparts. The one-step deposit (I) was most efficient as biofilm growth inhibitor in the dark.

It is quite clear that in one-step deposits silver addition increased the photocatalytic stearic acid- and biofilm removal efficiency. The reason for the lower activity of the two-step deposits comparing to the deposits made by one-step method is most probably due to the silver segregation on topmost layer of the samples prepared by the two-step method. This segregation layer can prevent the illumination penetration to the porous titania layer and therefore the photocatalytic activity decreases. The one-step deposits have also higher photocatalytic activity before loose material removing comparing to only titania deposits. Silver should increase the photocatalytic activity [16]. In this study also the decrease in particle size [12] in one-step samples can contribute to that, by increasing the specific surface area of the deposits. In photocatalytic activity test (table 2) the increase of activity from titania (sample E) and one-step titania (sample F) silver is so slight that it can induced by expected surface area growth. In bacteria test, the increasing is more clear (figure 4) and silver addition itself should have elevated also the photocatalytic activity of the deposit.

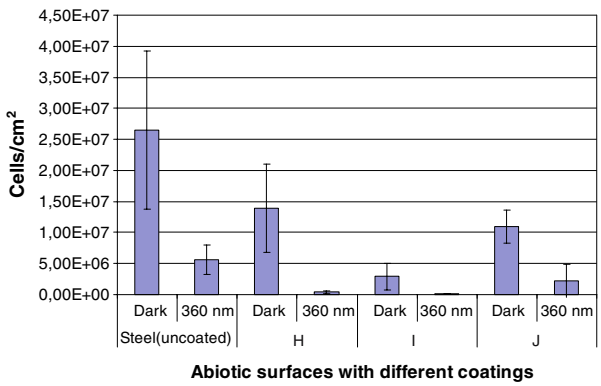

Figure 4. Densities of the biofilm bacterium *D. geothermalis* E50051 on stainless steel surfaces coated or not coated with titania (H), one-step titania-silver (I) and two-step titania-silver (J) deposits. The surfaces with biofilm were submerged in water and illuminated (24 h) or not illuminated at 360 nm. The biofilms on the surfaces were quantified using DNA/RNA specific fluorochrome staining. The staining results were converted to bacterial cell numbers by calibrating with known concentrations of *D. geothermalis* cells. Error bars display the variation from 2 to 4 coupons with biofilm.

4. Conclusions

Titania and titania-silver (1 wt%) deposits were generated by high temperature LFS technique. The deposits consisted of titania agglomerates made of ~10 nm primary particles. These agglomerates were covered by spherical silver particles (~2 nm). In the two-step method, silver was highly segregated on the topmost layer of the deposit. The photocatalytic activity was reasonably high for the deposited samples, which was attributed to the high surface area of the deposits. Titania and one-step titania-silver deposit was also active after cleaning the surface. The deposits have a capacity for photocatalytic biofilm removal and stearic acid destruction. Of the samples studied, the titania/silver deposits prepared by the one-step method have the highest potential as a photocatalyst.

Acknowledgments

This work was supported by Tekes (The National Technology Agency, Project Shine Pro/Pinta), Tampere University of Technology and Finnish Academy of Science and Letters. TEM and EDS analyses were performed by M. Sc. Tomi Kanerva, Institute of Material Science, Tampere University of Technology.

References

[1] S.E. Pratsinis, Prog. Energy Combust. Sci. 24 (1998) 197.
[2] S.H. Ehrman, S.K. Friedlander and M.R. Zachariah, J. Aerosol Sci. 29 (1998) 687.
[3] T. Johannessen and S. Koutsopoulos, J. Catal. 205 (2002) 404.
[4] H. Keskinen, J.M. Mäkelä, M. Vippola, M. Nurminen, J.K. Liimatainen, T. Lepistö and J. Keskinen, J. Mater. Res. 19 (2004) 1544.
[5] W.Y. Teoh, L. Mädler, D. Beydoun, S.E. Pratsinis and R. Amal, Chem. Eng. Sci. 60 (2005) 5852.
[6] H. Schulz, L. Mädler, R. Strobel, R. Jossen, S.E. Pratsinis T. Johannessen, J. Mater. Res. 20 (2005) 2568.
[7] W.J. Stark, J.D. Grunwaldt, M. Maciejewski, S.E. Pratsinis and A. Baiker, Chem. Mater. 17 (2005) 3352.
[8] R. Jossen, R. Mueller, S.E. Pratsinis, M. Watson and M.K. Akhtar, Nanotechnology 16 (2005) 609.
[9] D. Perednis, O. Wilhelm, S.E. Pratsinis and L.J. Gaukler, Thin Solid Films 474 (2005) 84.
[10] A. Teleki, S.E. Pratsinis, K. Wegner, R. Jossen and F. Krumeich, J. Mater. Res. 20 (2005) 1336.

[11] R. Strobel, S.E. Pratsinis and A. Baiker, J. Mater. Chem. 15 (2005) 605.
[12] H. Keskinen , J.M. Mäkelä, M. Aromaa, J. Ristimäki, T. Kanerva, E. Levänen, T. Mäntylä and J. Keskinen, to be published in Nanoparticle J. Res. in press (2006).
[13] A. Fujishima and K. Honda, Nature 238 (1972) 37.
[14] A. Fujishima, T.N. Rao and D.A. Tryk, J. Photochem. Photobiol C 1 (2001) 1.
[15] A. Mills, S. Le Hunte and J. Photochem, Photobiol. A: Chem. 108 (1997) 1.
[16] C. He, Y. Yu, X. Hu and A. Larbot, Appl. Surf. Sci. 200 (2002) 239.
[17] V. Vamathevan, R. Amal, D. Beydoun, G. Low and S. McEvoy, J Photochem. Photobiol.A: Chemistry (2002) 148–233.
[18] M.A. Mulligan, M. Wilson and J.C. Knowles, J. Biomed. Mat. Res. Part A. 67(2) (2003) 401.
[19] K. Wegner and S.E. Pratsinis, Powder Technol. 150 (2005) 117.
[20] J. Tikkanen, K.A. Gross, C.C. Berndt, V. Pitkänen, J. Keskinen, S. Raghu, M. Rajala and J. Karthikeyan, Surf. Coatings Technol. 90 (1997) 210.
[21] J.M. Mäkelä, S. Hellstén, J. Silvonen, M. Vippola, E. Levänen and T. Mäntylä, Mater. Lett. 60 (2006) 530.
[22] H. Keskinen, J.M. Mäkelä, S. Hellsten, M. Aromaa, E. Levänen and T. Mäntylä, Electrochem. Soc. Proc. Vol. 2005–09, 491.
[23] V. Pore, A. Rahtu, M. Leskelä, M. Ritala, T. Sajavaara J. Keinonen., Chem Vapor Dep. 10 (2004) 143.
[24] O.M. Väisänen, A. Weber, A. Bennasar, F.A. Rainey, H-J Busse and M.S. Salkinoja-Salonen, J. Appl. Microbiol. 84 (1998) 1069.
[25] Heterotrophic Plate Count. In: Clesceri LS, Greenberg AE, Eaton AD (eds) Standard Methods for the examination of water and wastewater, American Public Health Association, American Water Works Association and Water Environment Federation, 20th Edition, American Public Health Association, Washington DC, USA, 1992 9–34 to 9–36.
[26] K. Mattila, A. Weber and M.S. Salkinoja -Salonen, J Ind. Microbiol. Biotechnol. 28 (2002) 268.
[27] M. Raulio, V. Pore, S. Areva, M. Ritala, M. Leskelä, M. Lindén, J.B. Rosenholm, K. Lounatmaa and M. Salkinoja-Salonen, J Ind. Microbiol. Biotechnol. 33 (2006) 261.
[28] A. Mills and J. Wang, J. Photochem. Photobiol. A: Chemistry 182 (2006) 181.
[29] Y. Paz, Z. Luo, L. Rabenberg and A. Heller, J. Mater. Res. 10 (1995) 2842.
[30] Y. Paz and A. Heller, J. Mater. Res. 12 (1997) 2759.
[31] J.T. Remillard, J.R. McBride, K.E. Nietering, A.R. Drews X. Zhang, J. Phys. Chem. B 104 (2000) 4440.
[32] P. Sawunyama, L. Jiang, A. Fujishima and K. Hashimoto, J. Phys. Chem. B 101 (1997) 11000.
[33] S. Sitkiewitz and A. Heller, New J. Chem. 20 (1996) 233.